 CMC, vol.1, no.3, pp.275-288, 2004

Velocity Fluctuations in a Particle-Laden Turbulent Flow over a Backward-Facing Step

B. Wang[1], H.Q. Zhang[1], C.K. Chan[2] and X.L. Wang[1]

Abstract: Dilute gas-particle turbulent flow over a backward-facing step is numerically simulated. Large Eddy Simulation (LES) is used for the continuous phase and a Lagrangian trajectory method is adopted for the particle phase. Four typical locations in the flow field are chosen to investigate the two-phase velocity fluctuations. Time-series velocities of the gas phase with particles of different sizes are obtained. Velocity of the small particles is found to be similar to that of the gas phase, while high frequency noise exists in the velocity of the large particles. While the mean and rms velocities of the gas phase and small particles are correlated, the rms velocities of large particles have no correlation with the gas phase. The frequency spectrum of the velocity of the gas phase and the small particle phase show the -5/3 decay for higher wave number, as expected in a turbulent flow. However, there is a "rising tail" in the high frequency end of the spectrum for larger particles. It is shown that large particles behave differently in the flow field, while small particles behave similarly and dominated by the local gas phase flow.

keyword: Large eddy simulation, time series, frequency spectrum, two-phase turbulent flow, velocity fluctuation

1 Introduction

Two-phase turbulent flow is a fundamental phenomenon encountered widely in nature and in many engineering applications. In two-phase flow, while the particle motion is influenced by the gas phase, it is dependent on the momentum as well as on the characteristics time of the fluid fluctuations. Study on velocity fluctuations of the two phases is therefore important in understanding the effect of the gas phase on particle motion.

[1] Department of Engineering Mechanics
Tsinghua University, Beijing 100084, China
[2] Department of Applied Mathematics
The Hong Kong Polytechnic University

Most of the numerical simulation on two-phase turbulent flow has been focused on coherent structures of the gas phase and particle dispersion. Based on study on turbulent coherent structures of the single phase, particles dispersion by vortex structures in plane mixing layers has been investigated both experimentally and numerically by Crowe et al. (1988), Kamalu et al. (1988), Chien and Chung (1988) and Wen et al. (1992). Particles dispersion in axisymmetric jets has been investigated numerically by Chung and Troutt (1988) and Hansell et al. (1992). Tang et al (1990) presented numerical results of particle dispersion including the coupling effect in a developing plane shear layer. They reported the self-organized particle dispersion mechanism in free shear layers. Wei et al. (1998) used direct numerical simulation to study particle dispersion in a three dimensional temporal mixing layer. Lin et al. (2000) gave the regularity of particle motion during the process of vortex merging and studied the particle modulation to mixing layer which was also discussed by Wallner and Merbug (2002). Despite the relatively large amount of work on turbulent gas-particle flows, investigations on the characteristics of the velocity fluctuation of the two phases are still limited.

Generally, there are two kinds of numerical simulations in numerical studies on gas particle two-phase flow; namely the RANS method and the model-free simulation method. In the RANS method, velocity fluctuations of both phases are approximated by turbulence models, while the model-free simulation provides the instantaneous information of both phases to study the characteristics of two-phase velocity fluctuation.

In the model-free simulation, the gas phase can be numerically predicted by large eddy simulation (LES) or by direct numerical simulation (DNS). However, DNS is generally limited to low Reynolds number flow and is also extremely time consuming even on the most advanced super computers. Therefore, LES becomes a more effective approach for tackling complex turbulent

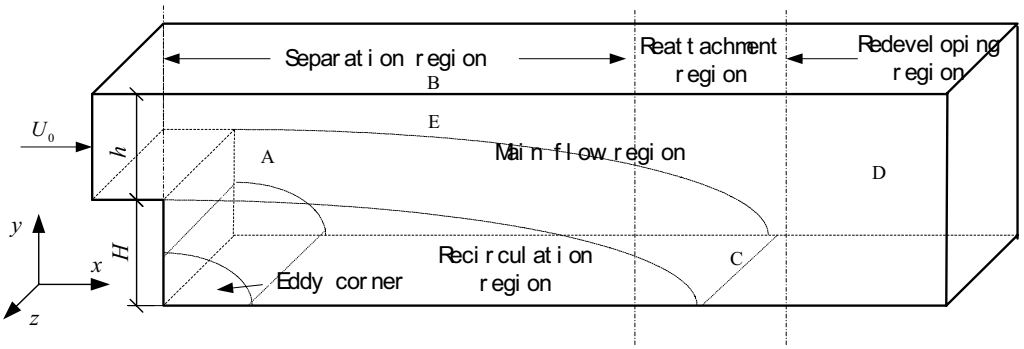

Figure 1 : Schematic diagram of the backward facing step

flows and studying instantaneous characteristics of the gas phase, , which can be carried out by finite difference method by Wang et al. (2004), finite element method by Shi and Paranjpe(2002) and Mai-Duy and Tran-Cong (2004) and meshless method by Lin and Atluri (2001).

Flow over a backward facing step is a typical flow occurring widely in many engineering applications. Recently, Wang et al. (2004) carried out successfully three-dimensional large eddy simulation of turbulent gas particle two-phase flow over a backward-facing step. Statistical results of mean and fluctuating velocities for the two phases agree well with experimental data. Energy spectrum of the gas phase also agrees well with turbulence theory as well as experimental measurements. Based on these results, the characteristics of velocity fluctuations of both phases are investigated in this paper.

2 Physical and numerical model

2.1 Flow configuration

In this paper, flow configuration for numerical simulation is shown in Fig. 1. The backward facing step height, $H$is 0.0267 m, which is used as the reference length scale. The channel height, h is 0.04 m, representing an expansion ratio of 5:3. The computational domain is $35H$, $2.5H$ and $10H$ in the streamwise, transverse and spanwise directions respectively. Reynolds number, Re_H based on the mean inlet velocity, $U_0$and step height, H is 18,400.

2.2 LES of gas-phase flows

In LES, each variable f is decomposed into two parts, one related to its large scale, $\overline{f}$, and the other related to its subgrid scale, f', i.e.

$$f = \overline{f} + f'. \tag{1}$$

The large scale is defined with the aid of a filter function G, such that

$$\overline{f}(x) = \int_D G(x - x')\, f(x')\, dx', \tag{2}$$

where D is the control volume. In this paper, G is the classical box filter used by Deardorff (1970) and Clark, Ferziger and Reynolds (1970) as

$$G(x - x') = \begin{cases} (1/\Delta)^3 , & |x_i - x_i'| \le (\frac{1}{2}\Delta) \\ 0 , & |x_i - x_i'| > (\frac{1}{2}\Delta) \end{cases} . \tag{3}$$

For the finite-volume discretization method used in this paper, the characteristic filter length is given by

$$\Delta = \left[\prod_{i=1}^{3} \Delta x_i \right]^{\frac{1}{3}}, \tag{4}$$

where Δx_i is the computational mesh size in the i-direction and the indices i = 1, 2, 3 refer to the streamwise, transverse and spanwise directions respectively.

Upon applying the filtering operation to the incompressible Navier-Stokes equations, the equations governing the motion of the resolved scales give

$$\frac{\partial \overline{u}_i}{\partial x_i} = 0, \tag{5}$$

$$\frac{\partial \overline{u}_i}{\partial t} + \frac{\partial}{\partial x_j}(\overline{u}_i \overline{u}_j) = -\frac{\partial p}{\partial x_i} + \frac{1}{Re_H} \frac{\partial^2 \overline{u}_i}{\partial x_j \partial x_j} - \frac{\partial \tau_{ij}}{\partial x_j} \tag{6}$$

The filtered equations have been made dimensionless using the step height H as length scale, the inlet velocity U_0 as velocity scale and the ratio of step height to inlet velocity as time scale. The Reynolds number in Eq.2 is given by $Re_H = U_0 H/\nu$, where ν is the kinematic viscosity. The velocity components for i = 1, 2 and 3 refer to the streamwise, transverse and spanwise directions respectively.

The resolved scales in the above equations interact with the unresolved scales via the sub-grid-scale (SGS) stress term, $\tau_{ij} = \overline{u_i u_j} + \overline{u}_i \overline{u}_j$, which is approximated by the eddy viscosity hypothesis

$$\tau_{ij} - \tfrac{1}{3}\delta_{ij}\tau_{kk} = -2\nu_T \overline{S}_{ij}, \tag{7}$$

where the eddy viscosity is defined as $\nu_T = C\Delta^2 \left|\overline{S}\right|$. The resolved-scale strain rate tensor is given by

$$\overline{S}_{ij} = \frac{1}{2}\left(\frac{\partial \overline{u}_i}{\partial x_j} + \frac{\partial \overline{u}_j}{\partial x_i}\right), \tag{8}$$

and $\left|\overline{S}\right| = \sqrt{2\overline{S}_{ij}\overline{S}_{ij}}$ is the magnitude of $\overline{S}_{ij}$. The model coefficient C requires specification in order to close the system (5) and (6). For empirical constant C in the SGS model, Deardorff (1970, 1971) suggested that C was taken as 0.1 in the turbulent channel flow. Schumann (1975) suggested C=0.17. But Poimelli and Moin (1988) suggested C=0.065. In this paper, C is taken as 0.13.

Eqs.5 and 6 are solved numerically using the fractional step method as described by Kim and Moin (1985) and Wu et al. (1995). Terms involving derivatives are approximated using second-order central difference for the viscous term and the advective term is discretized by a hybrid scheme using an upwind scheme with split coefficients and a second-order central difference scheme to reduce the aliasing errors and instability, which is discussed in detail by Kravchenko and Moin (1997). The momentum equations are integrated explicitly using a third-order Runge-Kutta algorithm and the Poisson equation for pressure is solved using series expansions in the streamwise and spanwise directions with tridiagonal matrix inversion.

The filtered equations are discretized spatially on a fully staggered Cartesian grid. For the computations in this paper, a uniform grid with 258 nodes in the stream-wise direction, 34 nodes in the transverse direction and 17 nodes in the spanwise direction is set up. The inlet flow condition is given by a uniform velocity distribution of $U(y)$ added with a random disturbance ξ, satisfying the normal distribution over the interval (-10^{-5},10^{-5}). 10^7 independent and randomly distributed data are used.

An improved non-reflective Sommerfeld open boundary condition, developed by Dai et al. (1994) is used at the outlet with the coherent structures transported downstream without any distortion. The velocity near the wall is calculated using a local dynamic wall model. In addition, periodic boundary conditions are used in the spanwise direction.

The first calculated point of velocity is not located in the viscous sub layer by using the local dynamic wall model. The total shear stress is assumed to be constant across the interval between the wall and the first mesh point and equal to the wall shear stress. The evaluation of the wall shear stress is based upon the assumption of a logarithmic velocity profile in the inertial sublayer of the turbulent boundary layer, defined by the local dynamic wall model

$$\overline{u} = u^* \left[\frac{1}{\kappa}\ln\left(\frac{y u^*}{\nu}\right) + 5\right]. \tag{9}$$

In addition, periodic boundary conditions are used in the spanwise direction.

2.3 Particle Motion

A Lagrangian approach is used to predict the properties of particles. The flow is assumed dilute and particle motion is simulated in the backward facing step without the influence of initial slip and gravity. The dominant force on each particle is thus the drag force.

The non-dimensional dynamic equations for a particle moving along its trajectory are

$$\frac{dX_p}{dt} = V_p, \tag{10}$$

$$\frac{dV_p}{dt} = \frac{F}{(1/6)\pi d_p^3 \rho_p}, \tag{11}$$

where V_p is the dimensionless instantaneous particle velocity. F is the drag force on the particle such that

$$F = C_d \cdot \frac{1}{4}\pi d_p^2 \cdot \frac{1}{2}\left|V_f - V_p\right|(V_f - V_p). \tag{12}$$

V_f is the instantaneous fluid velocity, C_d is the drag coefficient given by

$$C_d = \frac{24}{Re_p}\left(1 + \frac{Re_p^{2/3}}{6}\right) \quad , \quad 1 < Re_{\mathrm{p}} < 1000\,, \tag{13}$$

and $Re_{\mathrm{p}} = \frac{\rho |V_f - V_p| d_p}{\mu}$ is the particle Reynolds number and μ is the fluid viscosity.

The parameters in this paper are given in Tab. 1.

Table 1 : Parameters for the particle-laden flow

Gas phase (Air)	Particle phase
Reynolds number Re_H = 18,400	Mass loading Ratio < 5%
	$\rho_{\mathrm{p}} = 2,500\,\mathrm{kg/m^3}$
Initial average velocity U_0 = 10.5 m/s	d_{p} = 2μm, St=0.011
	d_{p} =200μm, St=111.184

3 Results and discussions

3.1 Turbulence statistics results and validation

It is of interest to evaluate the turbulence statistics results for which experimental results exist. After some times of numerical experiment, normal random inflow disturbances are imposed on gas phase flow and particle motion expediently. It is a correct treatment since we can gain good simulation results as analyzed below.

For the gas phase, the time-averaged mean velocities at central section of spanwise direction are obtained as

$$\overline{u}(x,y) = \sum_{i=n_0}^{n_1} u(x,y,i\Delta t)\Delta t / \sum_{i=n_0}^{n_1} \Delta t, \tag{14}$$

$$\overline{v}(x,y) = \sum_{i=n_0}^{n_1} v(x,y,i\Delta t)\Delta t / \sum_{i=n_0}^{n_1} \Delta t, \tag{15}$$

The fluctuating velocities is obtained as

$$u'(x,y) = \sum_{i=n_1}^{n_2} (u(x,y,i\Delta t) - \overline{u}(x,y))^2 \Delta t / \sum_{i=n_1}^{n_2} \Delta t, \tag{16}$$

$$v'(x,y) = \sum_{i=n_1}^{n_2} (v(x,y,i\Delta t) - \overline{v}(x,y))^2 \Delta t / \sum_{i=n_1}^{n_2} \Delta t \tag{17}$$

Where $u(x,y,i\Delta t)$ and $v(x,y,i\Delta t)$ are the instantaneous velocities in streamwise and transverse directions respectively, $\overline{u}(x,y)$ and $\overline{v}(x,y)$ are time-averaged velocity in streamwise and transverse directions respectively, Δt is the calculation time step.

For the particle phase, velocities are averaged over the control volume such that

$$\overline{u}_p = \sum_{i=1}^{N_p} u_{p,i}\tau_i / \sum_{i=1}^{N_P} \tau_i, \tag{18}$$

$$\overline{v}_p = \sum_{i=1}^{N_p} v_{p,i}\tau_i / \sum_{i=1}^{N_P} \tau_i, \tag{19}$$

$$u'_p = \sqrt{\sum_{i=1}^{N_p} (u_{p,i} - \overline{u}_p)^2 \tau_i / \sum_{i=1}^{N_p} \tau_i}, \tag{20}$$

$$v'_p = \sqrt{\sum_{i=1}^{N_p} (v_{p,i} - \overline{v}_p)^2 \tau_i / \sum_{i=1}^{N_p} \tau_i}, \tag{21}$$

where N_p is the number of particles passing through the control volumes, u_{pi} *and* $v_{p,i}$ are the instantaneous velocities of ith particle in streamwise and transverse directions respectively, $\overline{u}_p$ and $\overline{v}_p$ are their corresponding mean velocities, and u'_p and v'_p are their corresponding rms velocities, τ_i is the time at which particle i remains in the control volume.

Figure 2 shows the mean and fluctuating velocity profiles obtained from LES calculations as compared with experimental data. There is relatively poor agreement between the numerical results and the experiment data at the profile of X/H=2.0. Simulation shows the presence of a secondary recirculation region, which is not observed experimentally at the profile of that. For the undeveloped flow, the fluctuation gained from the inflow condition could be smaller than the experimental results. Except for these, simulations results are accepted successfully since the profiles agree well with the experimental data of Eaton and Johnston (1981).

Further comparisons were made between LES simulation and the experimental data of Eaton and Johnston for gas flow with 150 μm glass particles, having a Stokes number of 62.5. Figure 3 shows the mean and fluctuating velocity profiles obtained using LES as compared with experimental data. These numerical results are receivable in comparison with experiment data.

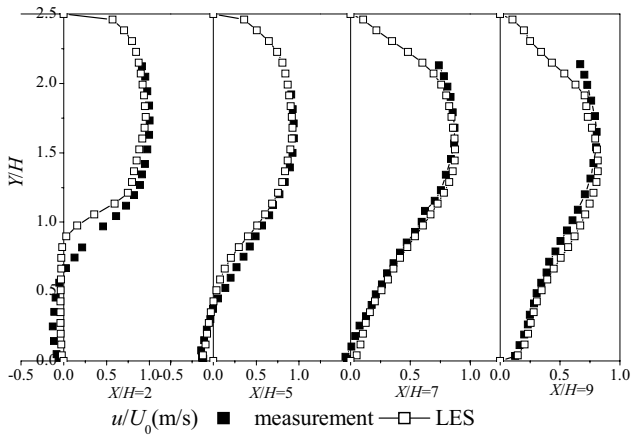

(a) Mean velocity in the streamwise direction

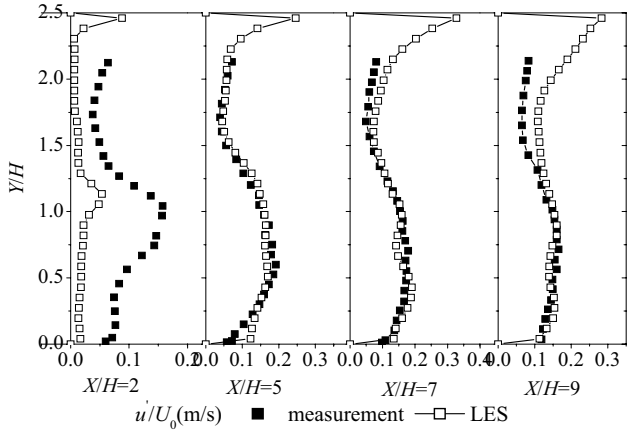

(b) Fluctuating velocity in the streamwise direction

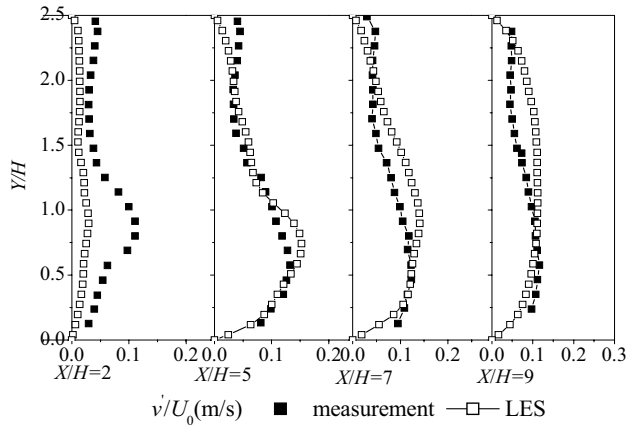

(c) Fluctuating velocity in the transverse direction

Figure 2 : mean and rms velocity of gas phase

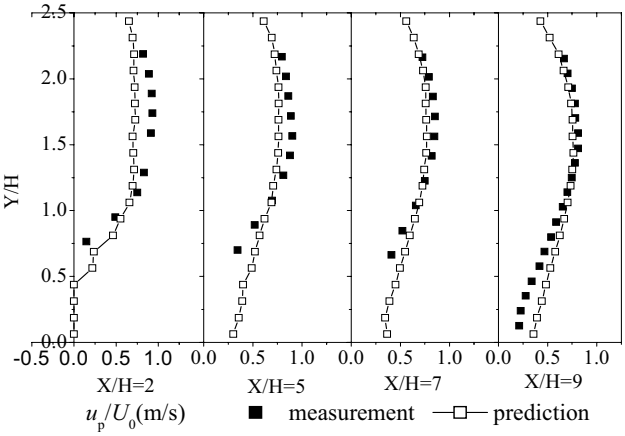

(a) Mean velocity in the streamwise direction

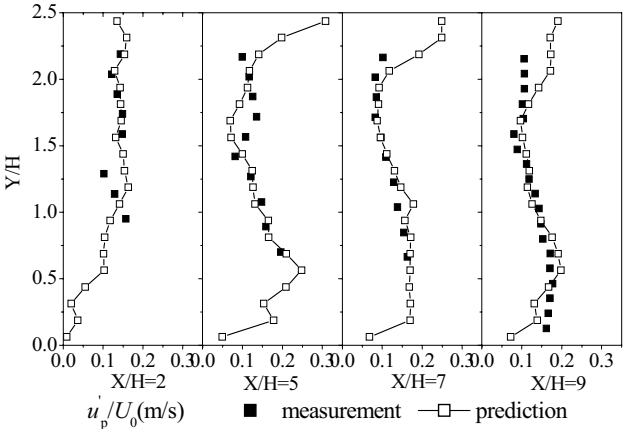

(b) Fluctuating velocity in the streamwise direction

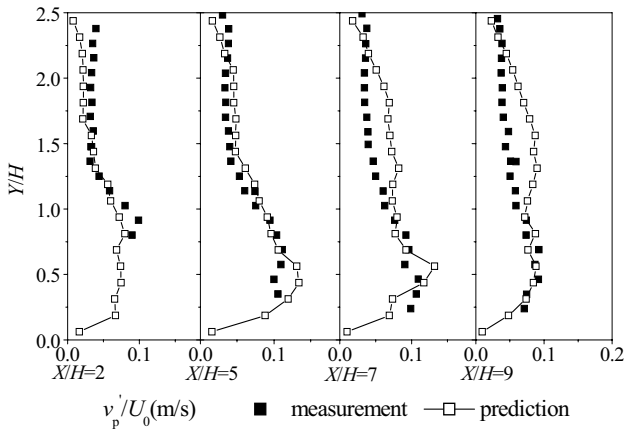

(c) Fluctuating velocity in the transverse direction

Figure 3 : mean and rms velocity of 150m glass particles

3.2 Instantaneous velocity for both phases

For the backward-facing step, four locations in the flow fields are selected as measuring points for two-phase velocity fluctuation as shown in Fig.1. Points A, B, C and D are in the shear flow region, the main flow region, the reattachment region and the redeveloping region respectively and instantaneous velocities of both phases at these locations are shown in Fig. 4 to Fig. 7.

In the shear flow region, the coherent structure including vortex roll up, growth and decay are induced by the large shear. The streamwise velocity variation is abrupt in this region. In the main flow region, the flow is still not disturbed by the expansion, and the streamwise velocity varies mildly and they are positive throughout. In the reattachment region, large coherent structures exist and the streamwise velocity varies significantly with reversed flow is evident. In the redeveloping region, the large vortices have broken up and many small vortices are present with large variations of streamwise velocity. In the shear flow region and reattachment region, the transverse velocities vary mildly, while their variations are abrupt with disturbance of small vortices, especially at location D.

Comparing velocity fluctuations of the two phases, there are significant differences for small particles of 2μm. It is difficult for large particles to penetrate into the reattachment region and velocity fluctuations of the 200μm particles cannot be analyzed correctly. The velocity fluctuations of 200μm particles at locations A, B and D are similar. Fig.4 to Fig.7 shows that the development of velocity fluctuation of the gas phase and 200μm particles are different. While the gas-phase velocities vary sharply within a wide range and are modulated by large and small vortices, the 200μm particles' velocities vary within a narrow range. The gas-phase velocity variations are induced by vortices and the 200μm particle velocity variations are mainly induced by structures of the particles. The transverse velocities of 2μm particles fluctuate with the same amplitude their streamwise velocities, while the transverse velocities of 200μm particles is very smaller than their streamwise velocities. It means that the large particles move in turbulent flow fields with a smooth trajectory in streamwise direction, while the trajectories of small particles in turbulent flow fields are much circuitously.

For small particles of 2μm, their velocity fluctuations are similar to that of the gas phase, especially in the downstream reattachment region and the redeveloping flow region. However, there are significant differences between the gas phase and 2μm particles in the phase angle of the velocity with low frequencies. This is mainly because large density particles, concentrated at the edge of small vortices, do not follow the gas-phase freely.

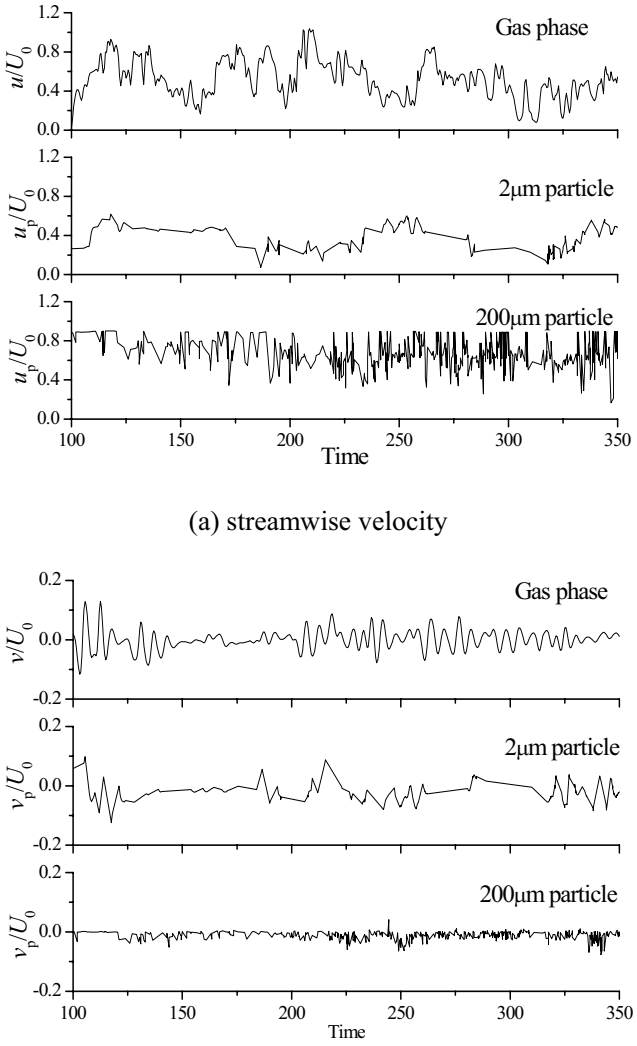

Figure 4 : time-series velocity for both phases at location A

3.3 Time-averaged properties for both phases

Mean and root mean square velocities at the four locations are shown in Fig.8. For small particles of 2μm, apart from the discrepancies in instantaneous velocities

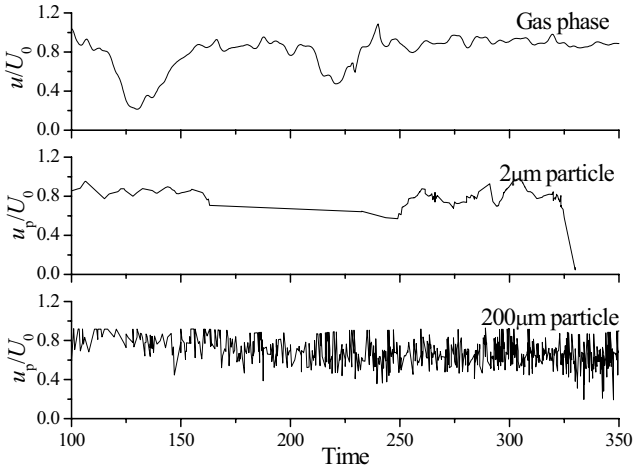

(a)Streamwise velocity

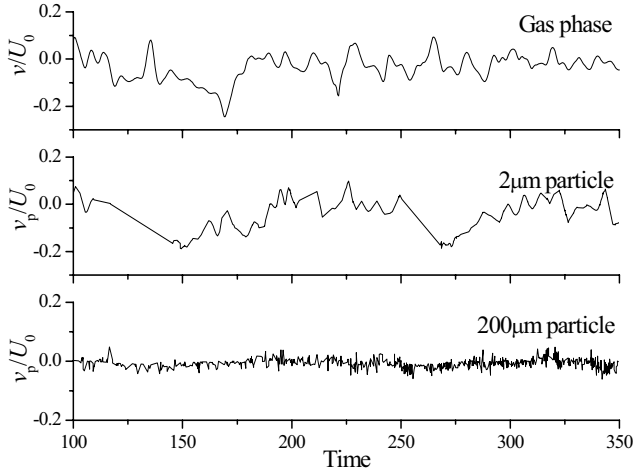

(b)Transverse velocity

Figure 5 : Time-series velocity for both phases at location B

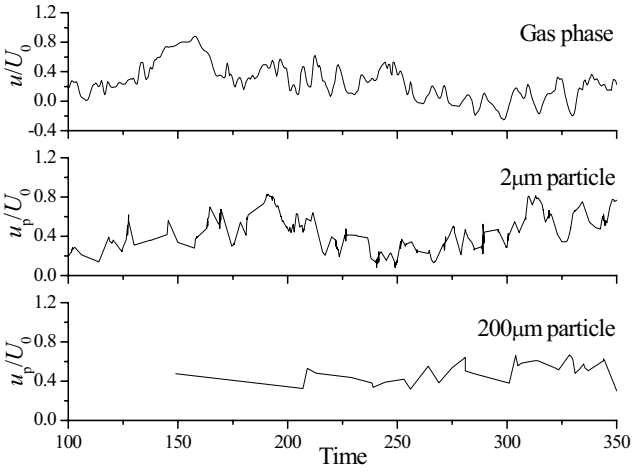

(a)Streamwise velocity

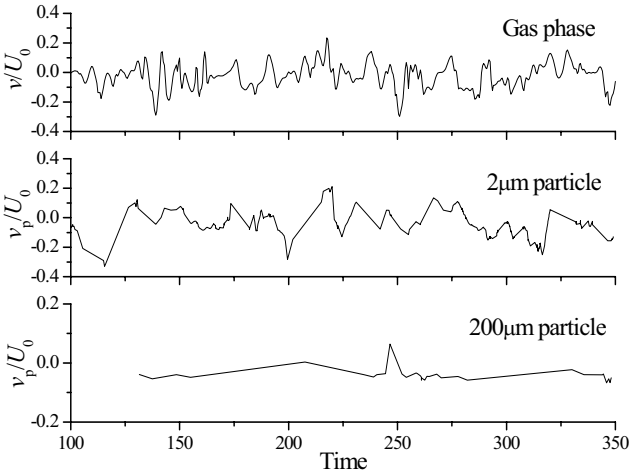

(b)Transverse Velocity

Figure 6 : Time-series velocity for both phases at location C

with the gas phase as shown in the last section, the mean and rms velocities are also different to that of the gas phase. And for large particles of 200μm, they are different significantly with both gas phase and small particles.

For streamwise velocities, comparing with particles of 2μm and 200μm, the effects of the gas-phase on the small particle is larger than on the large particles. The change of mean velocities at the four locations for the large particles is similar to that for the small particle. However, the change of rms velocities at the four locations for the large particle is not related to that of the gas phase. This indicates that the motion of small particles are influenced not only by mean properties of the gas phase but also by the fluctuating properties, while the motion of large particles are mainly influenced by mean properties of the gas phase.

For transverse velocity, mean velocities of gas phase as well as small and large particles are very small and approach to zero. The mean and rms velocities of both gas phase and small particles are very close each other, it is shown again that the motion of small particle are affected by both mean and fluctuating properties of gas phase. The mean and rms velocities of large particles are very small for all locations, and their changes among four locations are different with that of gas phase and small particles. So the mean and rms velocities in trans-

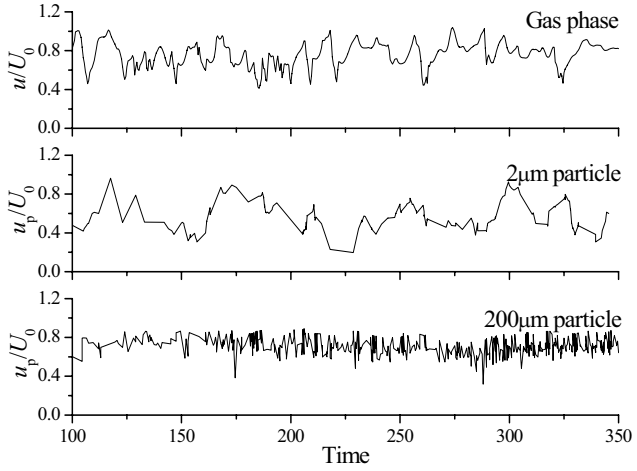

(a)Streamwise velocity

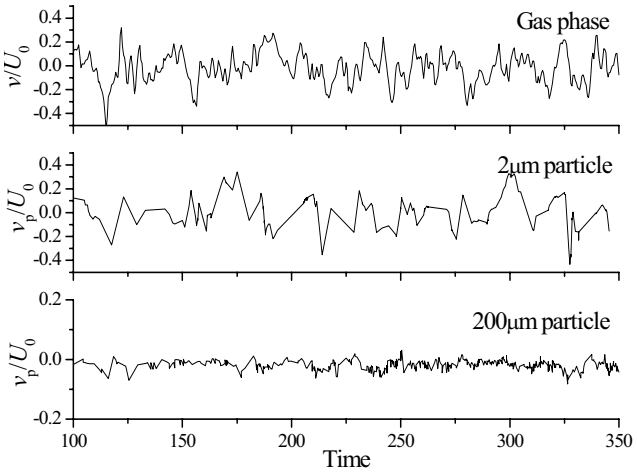

(b)Transverse velocity

Figure 7 : Time-series velocity for both phases at location D

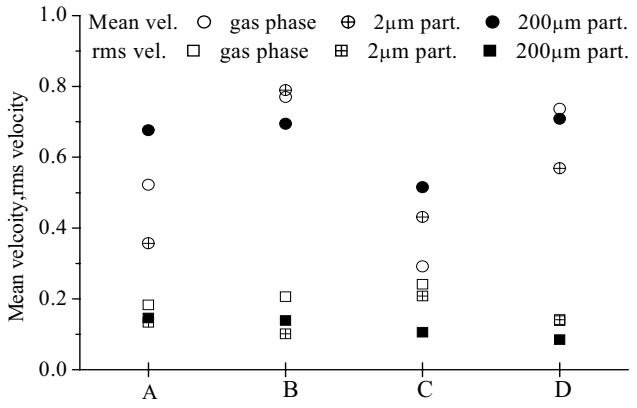

(a)Streamwise mean properties

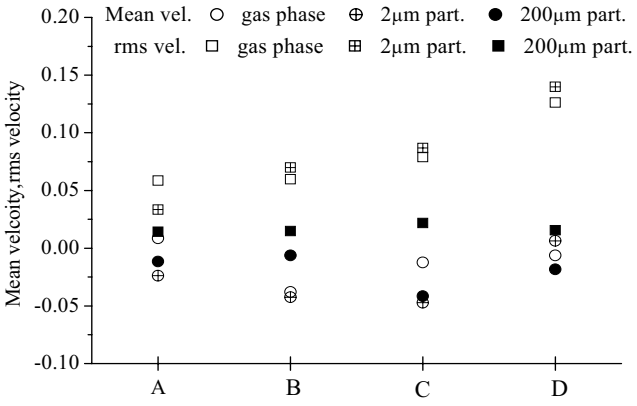

(b)Transverse mean properties

Figure 8 : Mean properties for both phases at the four locations

verse direction for large particles are less correlation to gas phase, which is contrary with that of the mean velocities in streamwise direction.

3.4 Frequency Spectrum for both phases

Fig.9 to Fig.12 shows the frequency spectrum of two-phase velocities at the four locations. The spectrum is obtained by Fast Fourier Transform of the autocorrelation of the velocity. The shapes of these gas-phase velocity spectra show the -5/3 decay for large wave numbers, as expected for turbulent flow. It indicates that the simulations of gas-phase turbulent flows by the current LES technique are suitable for differentiating the fluctuating property with low and high frequencies. The power increases with frequency in region of small wave number have been shown in frequency spectrum of transverse velocity, which are due to large vortex structure, while they are not clearly shown in that of streamwise velocities. The power of transverse velocity fluctuation is much less than that of streamwise velocity fluctuation

The frequency spectrum for the velocity of small particles is similar to the gas-phase velocity frequency spectrum. It can be seen that small particles follow the gas-phase closer than large particles although there is still some difference in the two frequency spectra.

It can be seen from Fig.9c, 10c, 11c and 12c that there is a “rising tail” distribution in the high frequency zone of spectrum of the large-particle velocity. The reason for

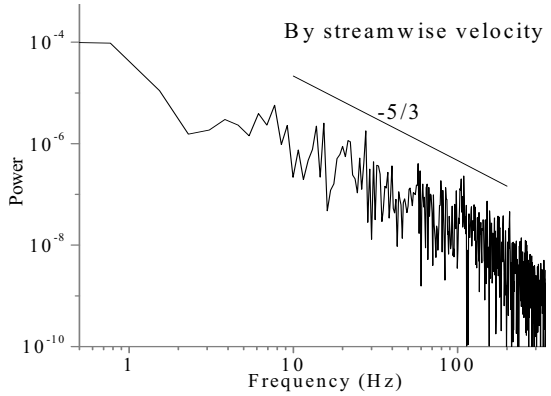

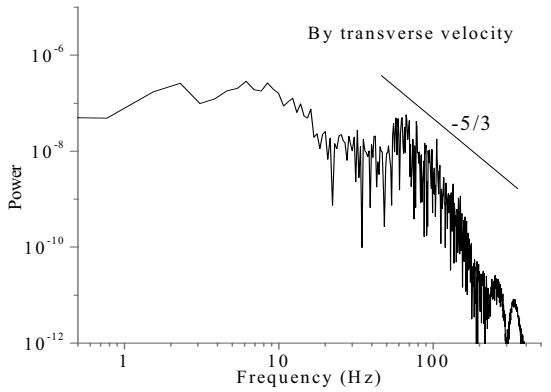

(a) Gas phase

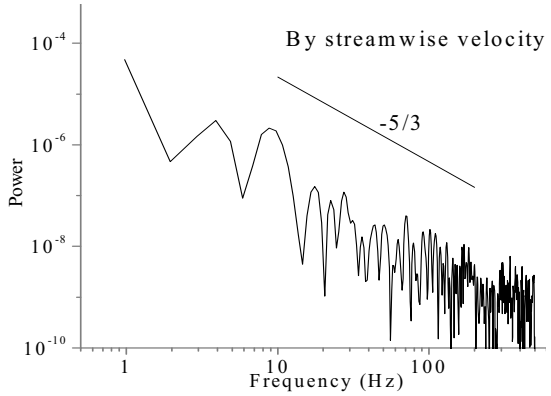

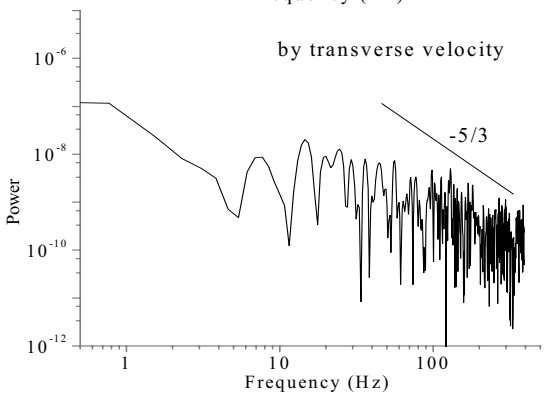

(b) Particle phase, for 2μm particles

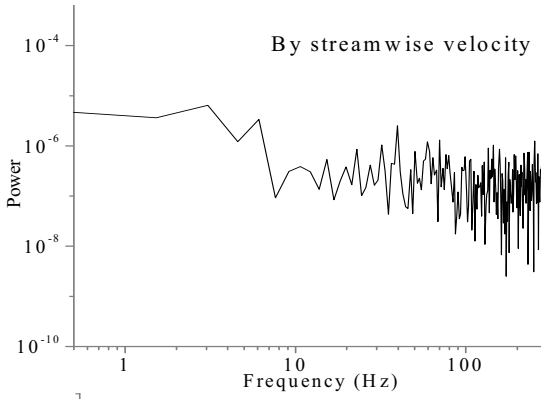

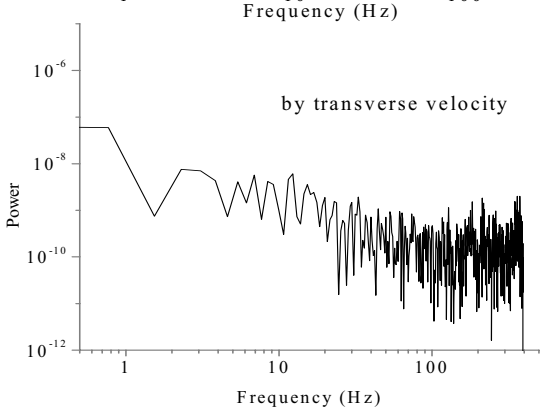

(c) Particle phase, for 200μm particles

Figure 9 : Frequency Spectrum for both phases at location A

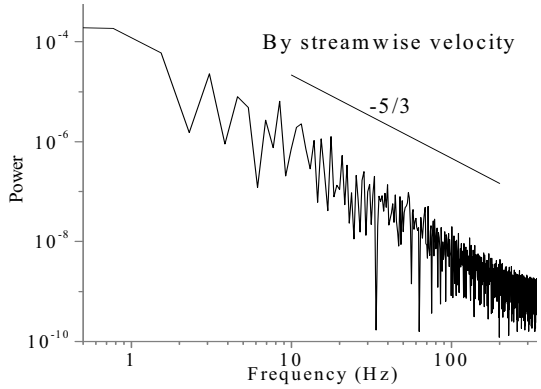

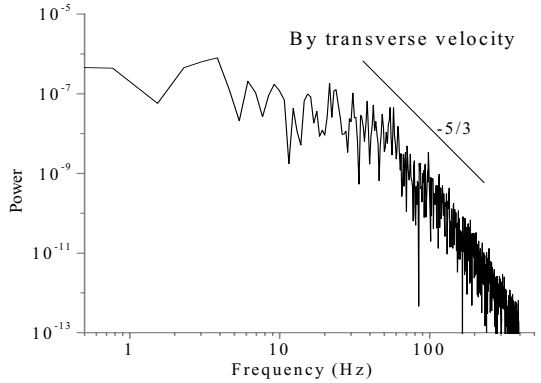

(a) Gas phase

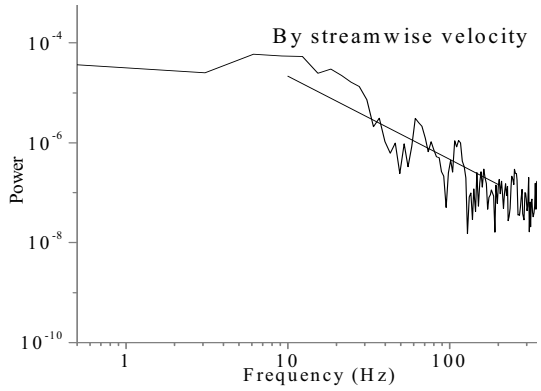

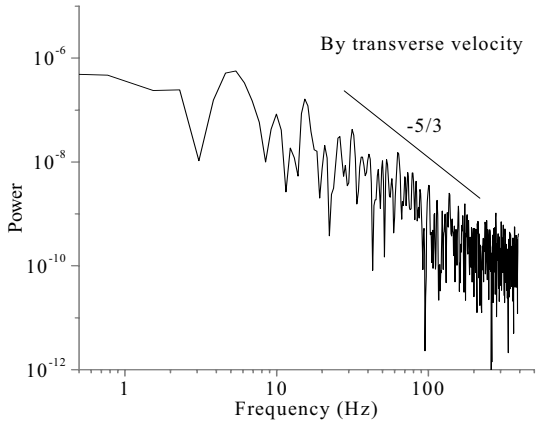

(b) Particle phase, for 2μm particles

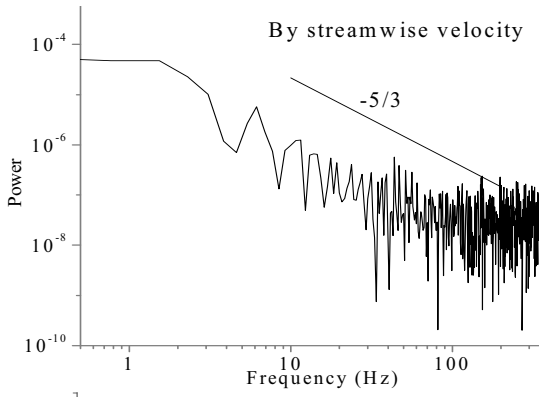

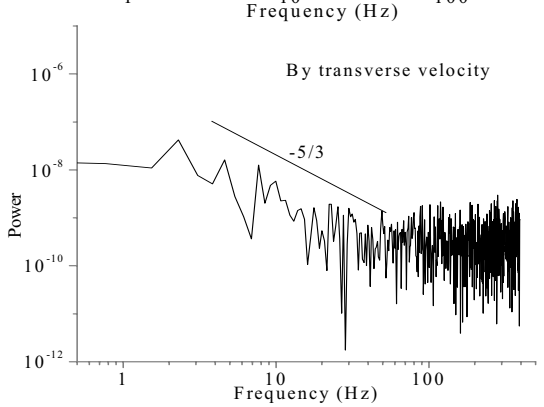

(c) Particle phase, for 200μm particles

Figure 10 : Frequency Spectrum for both phases at location B

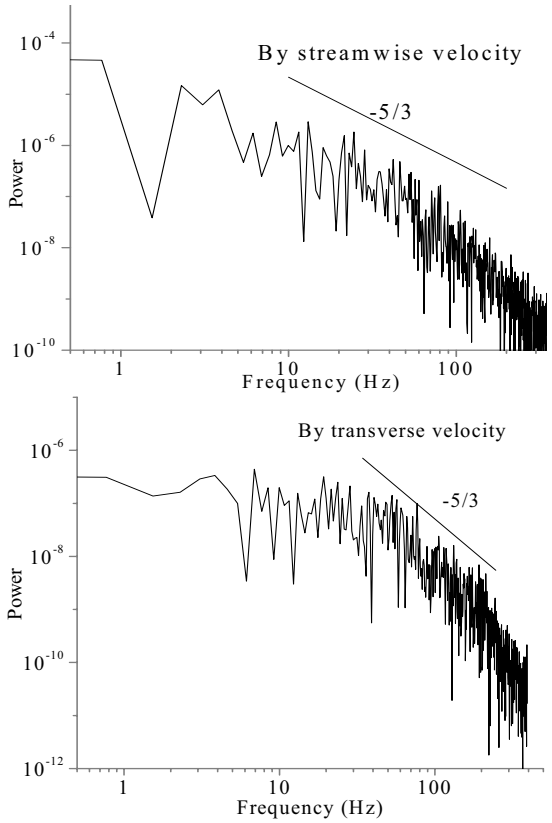

(a) Gas phase

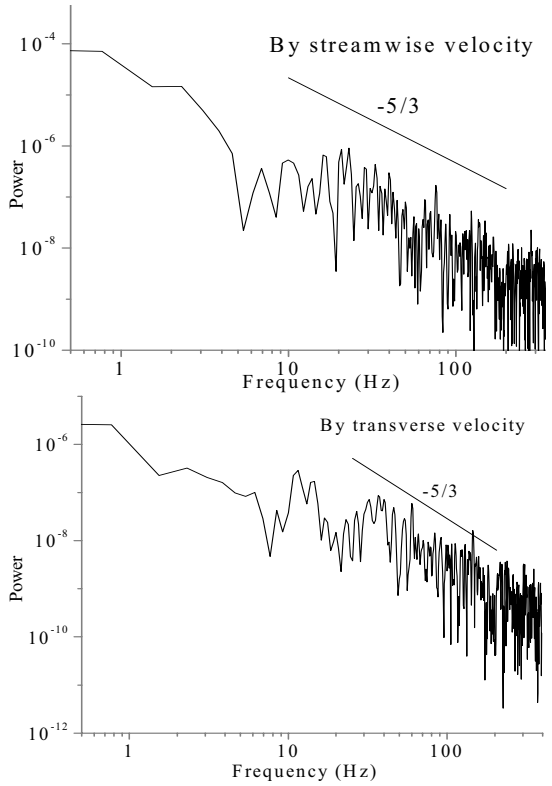

(b) Particle phase, for 2μm particles

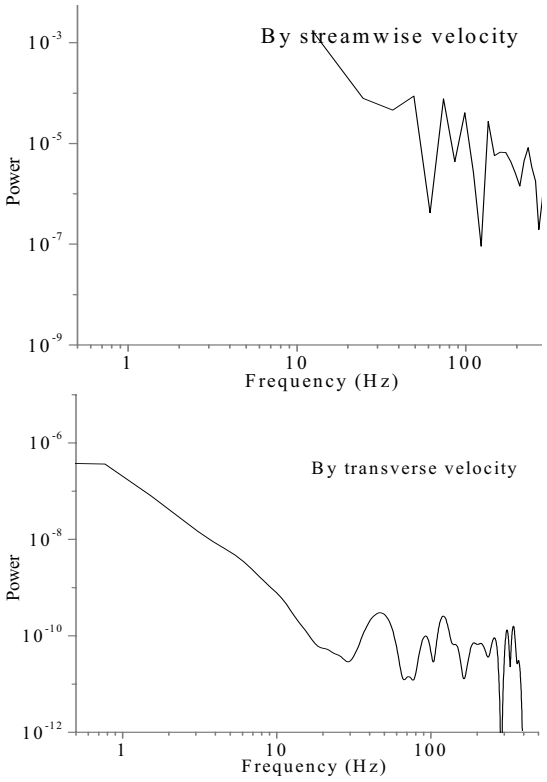

(c) Particle phase, for 200μm particles

Figure 11 : Frequency Spectrum for both phases at location C

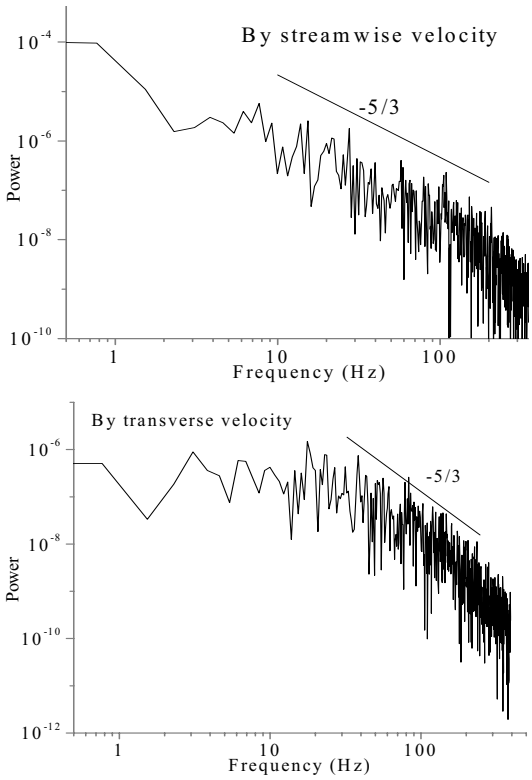

(a) Gas phase

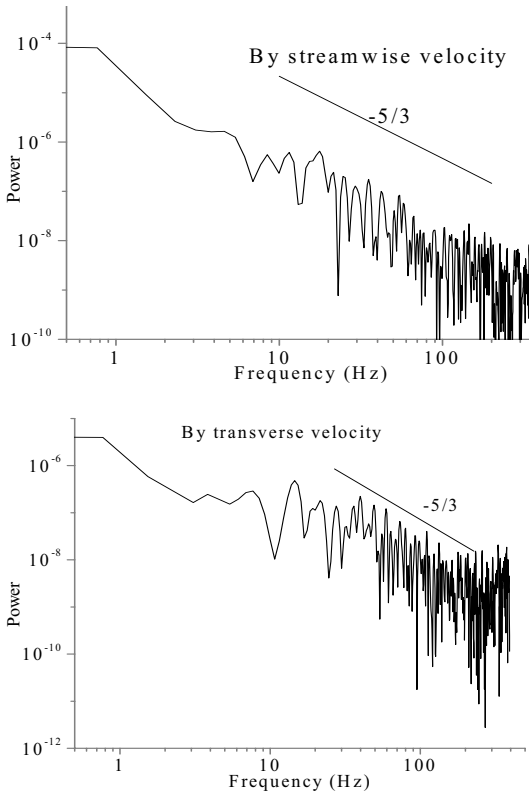

(b) Particle phase, for 2μm particles

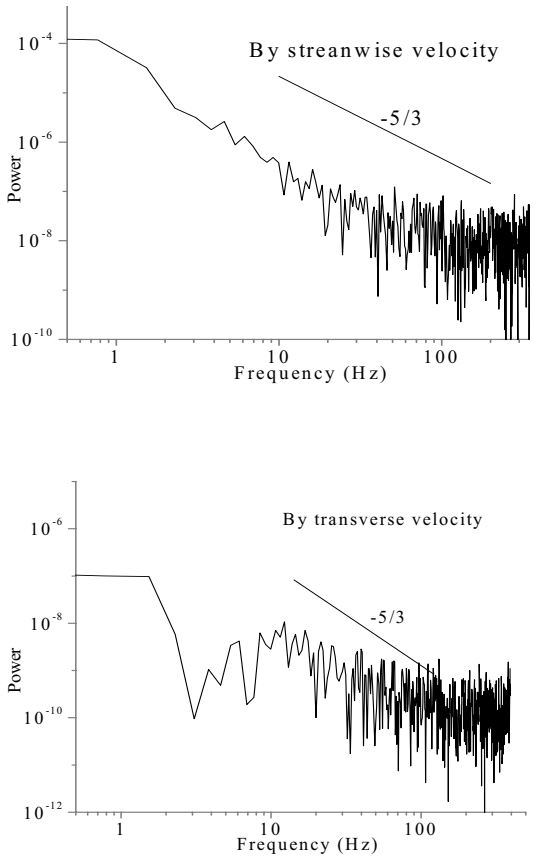

(c) Particle phase, for 200μm particles

Figure 12 : Frequency Spectrum for both phases at location D

such high frequency noise for the velocity of the large particles is that these large particles behave differently in the flow field. On the other hand, all the smaller particles behave similarly in the entire flow field and they are dominated by the local gas phase flow.

4 Conclusions

Velocity fluctuations of two phases are investigated at four typical locations in particle-laden flows over a backward-facing Step. Velocities of small particles are found to be similar to that of the gas phase, while there exist high frequency noise in the velocities for large particles. The mean and rms velocities of the gas phase and those for small particles are similar, while the rms velocities of large particles are different. The shape of the frequency spectrum of the gas phase and that of the small particle phase show the -5/3 decay for large wave numbers, while there is a "rising tail" in the high frequency end of the spectrum for large particles. It is shown that large particles behave differently in the flow field, while small particles behave similarly and dominated by the local gas phase. In addition, small particles respond to the mean and fluctuation properties of the gas phase, while large particles only respond to the mean properties of the gas phase.

Acknowledgement: This work was partially supported by the National Natural Science Foundation of China. (Grant Number 19972036&50176027) and the Research Committee of The Hong Kong Polytechnic University (Account Code G-T609).

References

Crowe, C. T.; Chung, J. N.; Troutt, T. R. (1988): Particle mixing in free shear flows. *Progress in Energy and Combustion Science*, vol. 14, pp. 171-194.

Chung, J. N.; Troutt, T. R. (1988): Simulation of particle dispersion in an axisymmetric jet. *Journal of Fluid Mechanics*, vol. 186, pp. 199-222.

Dai, Y.; Kogayashi, Y.; Taniguchi, N. (1994): Large eddy simulation of plane turbulent jet flow using a new outflow velocity boundary condition. *JSME International Journal Series B: Fluids Thermal Engineering*, vol.37, pp. 242-253.

Deardorff, J. W. (1970): A numerical study of three-dimensional turbulent channel flow at large Reynolds numbers. *J. Fluid Mech.*, vol. 41, pp. 453∼480.

Eaton, J. K.; Johnston, J. P. (1981): Review of research on subsonic turbulent flow reattachment. *AIAA Journal*, vol.19, pp. 1093-1100.

Hansell, D.; Kennedy, I. M.; Kollmann, W. (1992): A simulation of particle in a turbulent jet. *International Journal of Multiphase Flow*, vol. 18, pp. 559-576.

Kim, J.; Moin, P. (1985): Application of a fractional-step method to incompressible Navier-Stokes equations. *Journal of Computational Physics*, vol.59, pp. 308-323.

Kamalu, N.; Wen, F.; Troutt, T. R. (1988): Particle dispersion by ordered motion in turbulent mixing layers. *ASME Cavitation and Multiphase Flow Forum. FED* 64, pp. 150-154.

Kravchenko, A. G.; Moin, P. (1997): On the effect of numerical errors in large eddy simulations of turbulent flows. *Journal of Computational Physics*, vol.131, pp. 310-322.

Lin, H.; Atluri, S.N. (2001): The Meshless Local Petrov-Galerkin (MLPG) Method for Solving Incompressible Navier-Stokes Equations. *CMES: Computer Modeling in Engineering and Sciences*, Vol. 2, pp. 117-142.

Lin, J. Z.; Shi, X.; Yu, Z. (2000): Research on the effect of particle of two-dimensional shear flow. *Applied Mathematics and Mechanics*, vol. 21, pp. 855-860.

Mai-Duy, N.; Tran-Cong, T. (2004): Boundary Integral-Based Domain Decomposition Technique for Solution of Navier Stokes Equations. *CMES: Computer Modeling in Engineering and Sciences*, Vol. 6, pp. 59-76

Poimelli, U.; Moin, P.; Ferziger, J. H. (1988): Model consistency in large eddy simulation of turbulent channel flows. *Phys. Fluids,* vol. 31, pp.1884∼1891.

Schumann, U. (1975): Subgrid scale model for finite difference simulation of turbulent flows in plane channel and annuli. *J. Comp. Phys.*, vol. 18, pp. 376∼404.

Shi, F.; Paranjpe, R. (2002): An Implicit Finite Element Cavitation Algorithm *CMES: Computer Modeling in Engineering and Sciences*, Vol. 3, No. 4, pp. 507-516

Tang, L.; Crowe, C. T.; Chung, J. N. (1990): A numerical model for droplets dispersing in a developing plane shear layer including coupling effects. *Numerical Methods for Multiphase Flows*, *ASME FED*, 91, 27-33.

Wallner, E.; Merbug, E. (2002): Vortex pairing in two-way coupled, particle laden mixing layers. *International*

Journal of Multiphase Flow, vol. 28, pp. 325-346.

Wang, B.; Zhang H. Q.; Wang, X. L. (2004): Study on particle response to local fluid velocity in a gas particle turbulent flow. *ASME, HT-FED*, 51

Wei, L.; Chung, J. N.; Troutt, T. R. (1998): Direct numerical simulation of a three-dimensional temporal mixing layer with particle dispersion. *Journal of Fluid Mechanics*, vol. 358, pp. 61-85.

Wen, F.; Kamalu, N.; Chung, J. N.; Crowe, C. T.; Troutt, T. R. (1992): Particle dispersion by vortex structures in plane mixing layers. *Journal of Fluids Engineering – Transactions of ASME*, vol. 114, pp. 657-666.

Wu, X.; Squires, K. D.; Wang, Q. (1995): On extension of the fractional step method to general curvilinear coordinate systems. *Numerical Heat Transfer*, vol.27, pp. 175-194.